



Flexible Modular Armour for Protection Against the 5.56 × 45 mm SS109 Projectiles

Adam WIŚNIEWSKI*, Dawid PACEK

*Military Institute of Armament Technology,
7 Wyszyńskiego St., 05-220 Zielonka, Poland*

**corresponding author, e-mail: wisniewskia@witu.mil.pl*

Manuscript received July 01, 2014. Final manuscript received January 05, 2015

DOI: 10.5604/20815891.1157772

Abstract. The paper presents the results of the depth of penetration tests (*DOP*) and numerical simulations of the 5.56 × 45 mm SS109 projectile impact onto passive, layered armours placed on the armour backing material. Investigated passive layered armours (with dimensions 100 × 100 mm) were composed of polyester cover; soft ballistic aramid textile layers and Al₂O₃ ceramic tile placed inside rubberized aramid bag. The 5.56 × 45 mm SS109 projectile was stopped for 7-mm thick ceramic tile. In the final armour modular interlayer will be used and each module will have common area near its edges with neighbouring modules. Considering that for 7-mm thick ceramic tile, the areal density of armour equals 42.1 kg/m². To decrease the areal density of the modular armour to the value of 20÷30 kg/m² the numerical simulations with the use of the Ansys Autodyn v15 program were performed as the base for further *DOP* tests. One and two-layer armours with two kinds of ceramic tiles (Al₂O₃, SiC), armour steel plate (Armox 500) and titanium plate (Ti6Al4V) were investigated. The results of numerical simulation for the most effective armour for protection against the 5.56 × 45 mm SS109 projectile were presented.

Keywords: mechanics, body armour, 5.56 × 45 mm SS109 projectile, flexible modular armour, numerical simulation

This paper is based on the work presented at the 10th International Armament Conference on „Scientific Aspects of Armament and Safety Technology”, Ryn, Poland, September 15-18, 2014.

1. INTRODUCTION

Body armour to prevent internal organs injuries in addition to protection against perforation should be resistant to excessive blunt force trauma. In case of such armour, flexibility and low weight assuring freedom of movement for the user are of special importance.

For higher protection levels of body armours (e.g. K3÷K5 – according to Polish Standard PN-V-87000:2011, III÷IV – according to U.S. NIJ Standard-0101.06) hard ballistic plates (steel, ceramic, UHMWPE, composite, layered) are used (Fig. 1). They allow to stop projectiles with high kinetic energy (1.80÷3.96 kJ) however because of their rigidity they limit user freedom of movement.



Fig. 1. Hard ballistic plates used for higher protection levels (e.g. K3÷K5 according to Polish Standard PN-V-87000:2011) in modern body armours: a – steel plates [1]; b – ceramic plates [2]; c – UHMWPE plates [3]; d – layered armour [4]



Fig. 2. Modular interlayer used for lower protection levels (K2 according to Polish Standard PN-V-87000:1999; K1 according to Polish Standard PN-V-87000:2011) in the *Smart Armour* project

The aim of the experimental ballistic tests and the numerical simulations described in the paper was development of flexible armour for protection against 5.56 × 45 mm SS109 projectile on the base of the modular interlayer used in the project *Smart passive body armours with the use of rheological fluids with nano-structures* (UDA-POIG.01.03.01-00-060/08) for lower protection levels (K2 according to Polish Standard PN-V-87000:1999; K1 according to Polish Standard PN-V-87000:2011) and ceramic-composite layers.

2. EXPERIMENTAL TESTS OF 100 × 100 mm ARMOUR SAMPLES

The experimental ballistic tests of armour samples (100 × 100 mm dimensions) resistance against 5.56 × 45 mm SS109 projectile (impact velocity $V_i \approx 930$ m/s) were carried out. The used projectile consists of a brass jacket, steel core, and a lead core. The armour samples were fixed by two belts (loaded with 5 kg weight) to box with armour backing material. The test stand, the armour gripping, the cartridge and the cross-section of the projectile are shown in Figure 3.

Armour samples consisted of: rubberized aramid bag with Al_2O_3 ceramic tile and soft ballistic aramid layers of Kevlar XP®S307, placed in polyester cover.

The investigated Al_2O_3 ceramic tile was placed in the bag of 100 × 100 mm size glued from two layers of rubberized aramid. The empty space in a bag was filled with glue. Three kinds of bags with ceramic tile: 6-mm, 7-mm, and 8-mm thick were made. Other dimensions of ceramic tiles in all cases were the same and equalled to 50 × 50 mm (Fig. 4).

Results of the ballistic tests are shown in Table 1. Deformations (damages) of armour and backing material are shown in Figures 5÷7. Measuring of any values which could describe the deformed projectile was not possible because the projectile fragmented into very fine elements.

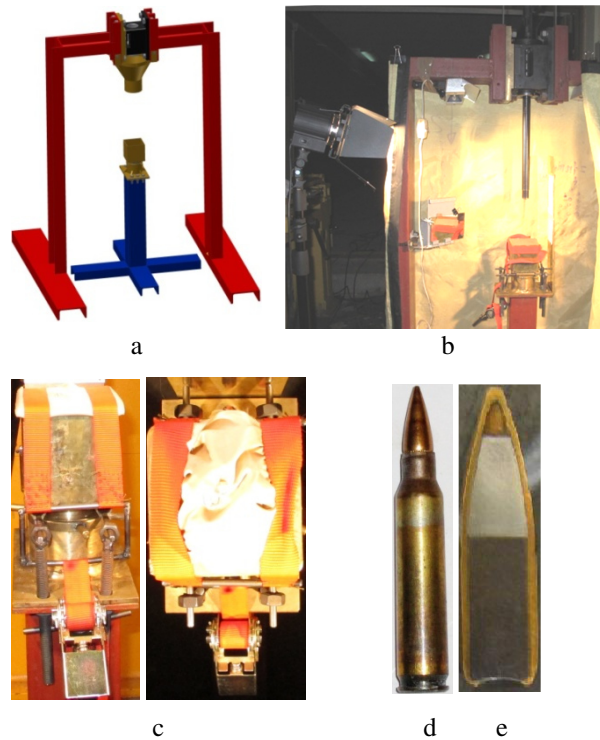


Fig. 3. Stand for the ballistic test: a – CAD model of stand; b – real stand; c – armour gripping; d – projectile 5.56 × 45 mm SS109; e – cross-section of the 5.56 × 45 mm SS109 projectile [5]

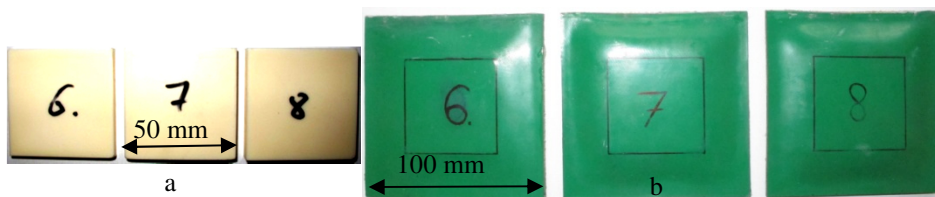


Fig. 4. Rubberized aramid bags with ceramic tiles: a – Al_2O_3 ceramic tiles; b – rubberized aramid bags with ceramic tiles inside

The 6.5-mm thick armour steel plate (50.7 kg/m^2 areal density) of 500 HB hardness stops the used for tests 5.56 × 45 mm SS109 projectile [6]. In case of the 5.56 × 45 mm SS109 projectile impact onto samples with aramid layers of Kevlar XP[®]S307 and bag with ceramic tile, stopping was achieved for a sample with areal density equal to 16.4 kg/m^2 (sample with 7 mm thick ceramic tile).

Table 1. Results of the ballistic tests (5.56 × 45 mm SS109 projectile of impact velocity 930 m/s)

Sample No.	Armour	Armour mass, m_u , mass of bag with ceramic $\{m_{CA}\}$, g	Result, P/S^1	Backing material deformation		Number of perforated layers
				Backface Signature, BFS , mm	Diameter of indentation, ϕ_{min} / ϕ_{max} , mm	
1	3 w. Kev.XP S307 / WGA CA8 / 10 w. Kev.XP S307	174 {130}	<i>S</i>	19	55 / 70	3 + ceramic tile
2	3 w. Kev.XP S307 / WGA CA7 / 10 w. Kev.XP S307	164 {119}	<i>S</i>	21	68 / 78	3 + ceramic tile
3	3 w. Kev.XP S307 / WGA CA6 / 10 w. Kev.XP S307	149 {106}	<i>P</i>	—	—	all

P – armour perforation; *S* – projectile stopping

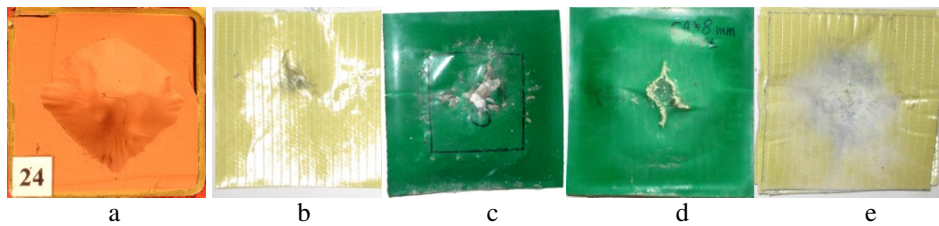


Fig. 5. Sample No. 1 (8 mm thick ceramic tile), elements after ballistic test:
 a – backing material after level compensation; b – perforated layers;
 c – bag with the ceramic tile (front); d – bag with the ceramic tile (back);
 e – non perforated layers placed behind the bag

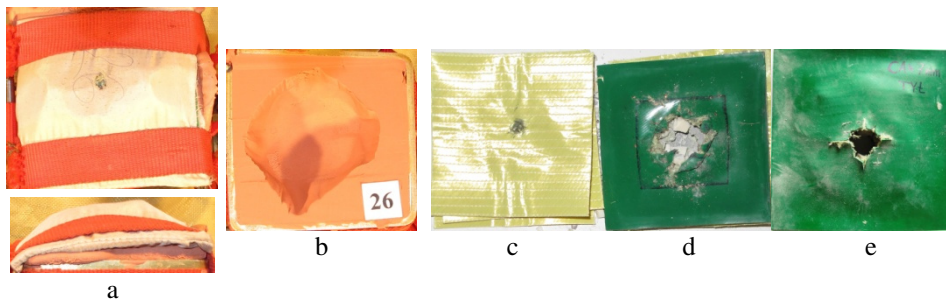


Fig. 6. Sample No. 2 (7 mm thick ceramic tile), elements after ballistic test:
 a – sample; b – backing material after level compensation; c – perforated layers;
 d – bag with the ceramic tile (front); e – bag with the ceramic tile (back)

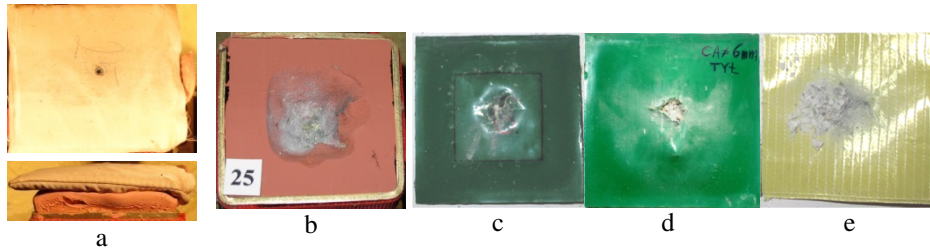


Fig. 7. Sample No. 3 (6 mm thick ceramic tile), elements after ballistic test: a – sample; b – backing material after level compensation; c – bag with the ceramic tile (front); d – bag with the ceramic tile (back); e – non perforated layers placed behind the bag

In comparison to the armour steel plate the achieved areal density of the armour during tests was about 68% smaller. In the final armour the ceramic tile will cover the entire area inside the bag, not only 25% of it. Furthermore, in case of using modular interlayer outermost areas of the bags will cover one another. Eventually, armour areal density will be equal to 42.1 kg/m^2 . In comparison to the armour steel plate it is about 17% smaller value, however in comparison to modern composite-layered armours – about 24÷68% greater.

With regard to the used now modern armours the advantages of the proposed armour are as follows:

- flexibility – ensuring more freedom of movement for the user;
- modularity – providing the possibility of quick replacement of damaged armour elements.

In case of the proposed armour for protection against the $5.56 \times 45 \text{ mm}$ SS109 projectiles, decrease in its mass is necessary. For this purpose, numerical simulations as the basis for further ballistic tests were carried out.

3. NUMERICAL SIMULATIONS

3.1. Numerical model of the projectile

$5.56 \times 45 \text{ mm}$ SS109 projectile consists of the brass jacket, the steel core, and the lead core. Material parameters values of equations of state, strength and failure models were adopted on the basis of the literature data [5, 7÷10] and from the Autodyn v15 program library database.

The correctness of the numerical model was verified on the basis of the literature ballistic test results of the $5.56 \times 45 \text{ mm}$ SS109 projectile impact onto 6.5 mm thick armour steel plate of 500 HB hardness (Thyssen-Krupp Secure 500). Material parameters obtained by experimental tests with the use of Split Hopkinson Pressure Bar were given in [6].

During ballistic tests [6] the ballistic velocity limit was achieved, defined as the velocity at which the bullet is expected to perforate the armour with 50% probability, equal to $V50 = 1003$ m/s.

For materials of the projectile jacket and core, and for the armour the Johnson–Cook strength model was applied. This model is described by the following equation:

$$\sigma = [A + B\varepsilon^n] \cdot [1 + C \ln \dot{\varepsilon}^*] \cdot [1 - T^{*m}] \quad T^* = \frac{T - T_p}{T_t - T_p} \quad (1)$$

where: σ – yield stress, A – static yield stress, B – strain hardening coefficient, n – strain hardening exponent, C – strain rate coefficient, m – thermal softening exponent, T^* – homologous temperature, T – temperature, T_p – room temperature, T_t – melting temperature, ε – equivalent plastic strain, $\dot{\varepsilon}^* = \varepsilon/\varepsilon_0$ – dimensionless plastic strain rate.

For the armour and the projectile materials (except for lead) the Johnson–Cook failure model was adopted, based on the accumulation of plastic strain. This failure criterion assumes the damage parameter D given by:

$$D = \sum \frac{\Delta\varepsilon}{\varepsilon^f}; \quad \varepsilon^f = [D_1 + D_2 e^{D_3 \sigma^*}] \cdot [1 + D_4 \ln |\dot{\varepsilon}^*|] \cdot [1 + D_5 T^*] \quad (2)$$

where: D_1, D_2, D_3, D_4, D_5 – material constants; $\sigma^* = \frac{p}{\bar{\sigma}}$ – pressure/stress measureless dependence; p – pressure; $\bar{\sigma}$ – equivalent of the von Mises' stress; $\Delta\varepsilon_p$ – increment of the effective plastic strain ε^f – equivalent plastic strain at cracking. The failure occurs when the parameter D achieves a value 1.

Material parameters adopted in the numerical simulations are shown in Table 2.

Table 2. Material parameters used in numerical simulations

Material	Johnson–Cook strength model					Johnson–Cook failure model				
	A , GPa	B , GPa	C	n	m	D_1	D_2	D_3	D_4	D_5
Steel	0.792	0.51	0.014	0.26	1.03	0.05	3.44	-2.12	0.002	0.61
Brass	0.112	0.505	0.009	0.42	1.68	0.54	4.89	-3.03	0.014	1.12
TKS500	1.3	2.23	0.045	0.559	0.96	0.168	0.035	-2.44	-0.045	0.919

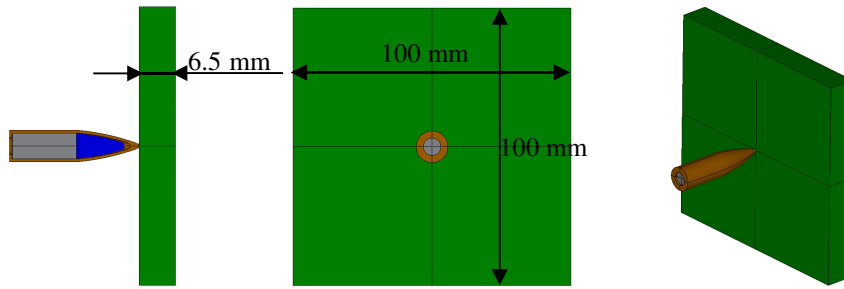


Fig. 8. Numerical model of the 5.56 × 45 mm SS109 projectile impact onto the steel armour

Time, t	14 μ s	40 μ s	60÷76 μ s	
Projectile impact velocity, V_i			60 μ s	
950 m/s				
1003 m/s			76 μ s	
1020 m/s			60 μ s	
	Cross section view of the projectile and the armour			The armour front view

Fig. 9. Numerical simulations of three variants of the projectile impact velocity at chosen points of time

In the performed numerical simulations (Fig. 8), the results conforming to those from literature ballistic tests were achieved. For velocity of the projectile impact onto the armour $V_i = 950$ m/s, the projectile was stopped, for velocity $V_i = 1020$ m/s, the armour was perforated and for velocity of the projectile impact equal to ballistic limit ($V_i = V_{50} = 1003$ m/s) the projectile was stopped and the armour was strongly deformed (cracking of the armour without perforation) (Fig. 9).

3.2. Numerical model of the armour backing material

Before the ballistic tests, plasticity of the armour backing material was investigated by triple drop tests of 1 kg steel weight (spherically ended cylinder of $\varphi = 44$ mm diameter) from 2-m altitude. Average value of indentation in the backing material equalled 20 mm. On the basis of the literature data and own experimental tests (steel weight free drop test) the previously developed by the authors [11] numerical model of the armour backing material was modified according to currently achieved results of steel weight drop tests. In the performed numerical simulations, backing material indentation equal to 20 mm was obtained, confirming the experiment.

The parameters selected and used in numerical simulations for armour backing material are given in Table 3, the result of numerical simulation is shown in Figure 10.

Table 3. Selected parameters of the armour backing material

Density, ρ , g/cm ³	1.56
Young's modulus, E , MPa	3
Shear modulus, G , MPa	1.007
Bulk modulus, K , MPa	50
Yield stress, A , MPa	0.065
Hardening constant, B , MPa	0.6
Hardening exponent, n	0,6
Thermal softening exponent, m	1
Poisson ratio, ν	0.49
Thermal conductivity, J/(m ³ K*s)	0.6
Heat capacity, J/(kg*K)	1280

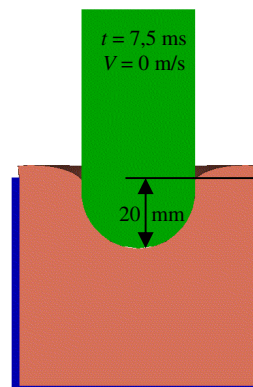


Fig. 10. Numerical result of steel weight drop test onto armour backing material

3.3. Numerical model of Kevlar XP S307

Soft ballistic aramid Kevlar XP®S307 consists of two layers in a criss-cross (0/90°) orientation of aligned in the same direction filament fibres and is sewed every 5 mm by string bead oriented at the angle of 45° to the fibres directions.

These types of composites (laminates) are represented in numerical simulations by: overall replacement model, layered replacement model or micro-mechanical replacement model.

In comparison to overall replacement model the layered replacement model allows for more detailed modelling of delamination phenomena and for consideration of different laminas orientation to each other. Micro-mechanical replacement model gives the possibility of modelling fibre slip and fibre-to-matrix interactions.

In case of the 5.56×45 mm SS109 projectile penetration into loosely arranged layers of soft ballistic type of aramid Kevlar XP®S307, delamination of single layers was not observed. Therefore, considering additionally small thickness of a single layer ($t = 0.3$ mm) in the numerical simulations described in the present article, the overall replacement model for aramid Kevlar XP®S307 was adopted.

Soft ballistic aramid layers of Kevlar XP®S307 were described with the use of orthotropic equation of state.

In the numerical simulations orthotropic failure model was adopted. In this model influence of damage mechanisms such as delamination, matrix cracking, fibre failure, and through laminate thickness and shear strains are considered as a single phenomenon – softening. Together with failure initiation material stresses are not reduced to zero instantaneously but linearly in a function of so-called crack strain ε^{cr} (Fig. 11).

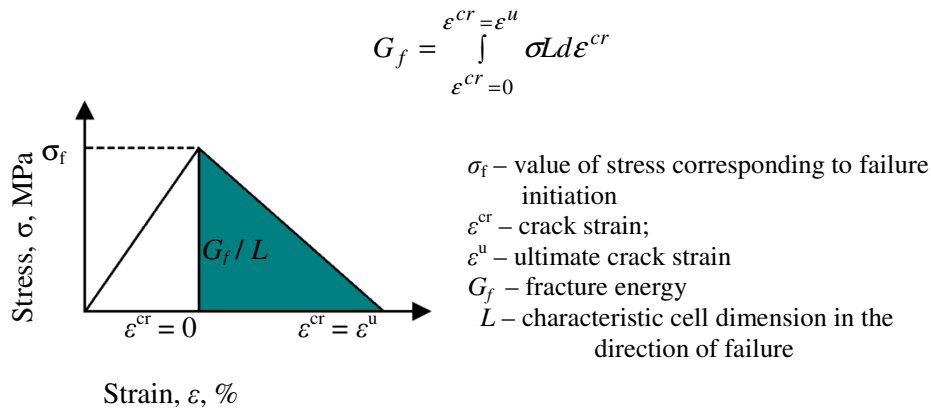


Fig. 11. Schema of the softening algorithm

The area under the stress-strain curve connected with the material softening is dependent on material property described as the fracture energy G_f and on the characteristic cell dimension in the direction of failure.

3.4. Numerical model of ceramic tile

For ceramic tiles description the Johnson–Holmquist model was adopted. The model distinguishes two material strength limits σ_i^* and σ_f^* , respectively, for intact and fractured material. Dependence between them, pressure and strain rate are as follows:

$$\sigma_i^* = A(t^* + p^*)^N (1 + C \ln \dot{\varepsilon}^*); \quad \sigma_f^* = B(p^*)^M (1 + C \ln \dot{\varepsilon}^*) \quad (3)$$

where: A – intact strength constant; B – fractured strength constant; N – intact strength exponent; M – fractured strength exponent; C – strain rate constant; $\dot{\varepsilon}^*$ – maximum fracture strength ratio;

$$t^* = \frac{T}{p_{hel}}; \quad p^* = \frac{P}{p_{hel}}; \quad \dot{\varepsilon}^* = \frac{\dot{\varepsilon}}{\dot{\varepsilon}_0} \quad (4)$$

and T – tensile strength; P – current pressure; p_{HEL} – pressure at Hugoniot Elastic Limit; $\dot{\varepsilon}_0$ – reference strain rate.

The current material strength with respect to its damage D is determined from the equation:

$$\sigma^* = \sigma_i^* - D(\sigma_i^* - \sigma_f^*) \quad (5)$$

where:

$$D = \sum \frac{\Delta \varepsilon^p}{\varepsilon_f^p}; \quad \varepsilon_f^p = d_1(p^* + t^*)^{d_2} \quad (6)$$

and: ε_f^p – strain to fracture; d_1 – fracture coefficient; d_2 – fracture exponent.

Relation between density and pressure in the ceramic material was described by polynomial equation of state which in case of compression takes the form:

$$p_{hel} = k_1 \mu_{hel} + k_2 \mu_{hel}^2 + k_3 \mu_{hel}^3 \quad (7)$$

where: k_1, k_2, k_3 - material constants and $\mu_{hel} = \frac{\rho_{hel}}{\rho_0} - 1$

ρ_0 – initial density; ρ_{hel} – density at Hugoniot Elastic Limit.

3.5. Numerical simulation of the 5.56×45 mm SS109 projectile impact onto the composite armour

In the first order the numerical simulation of the 5.56×45 mm SS109 projectile impact onto the armour responding to the one used during the experimental ballistic tests (100×100 mm size of soft ballistic aramid layers of Kevlar XP[®]S307 added to the $50 \times 50 \times 7$ mm size Al_2O_3 ceramic tile placed inside the 100×100 mm size aramid bag, described in section 2) was performed. The numerical model of the bag with the ceramic tile is shown in Figure 12.

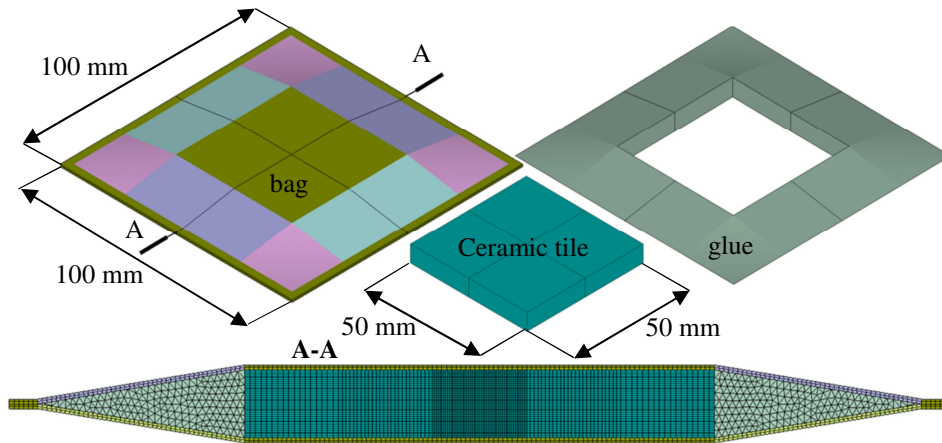


Fig. 12. Numerical model of the bag with the ceramic tile and glue

The material parameters for Al_2O_3 ceramics were adopted on the basis of the literature [12÷14] and Autodyn v15 library database.

The obtained results of the performed numerical simulations are shown in Figure 13. The projectile stopping conformed to the results of ballistic tests.

In the second part of the numerical analyses, the simulations of the 5.56×45 mm SS109 projectile impact ($V_i = 900$ m/s) onto various armours, placed inside the aramid bag, were performed. One- and two-layer armours were selected in such a way that the areal density of the final armour with a modular interlayer (Fig. 2) equalled to $m_{ma} = 20 \div 30$ kg/m². Armours with two kinds of ceramic tiles (Al_2O_3 , SiC), armour steel plate (ArmoX 500) and titanium plate (Ti6Al4V) were investigated (Table 4).

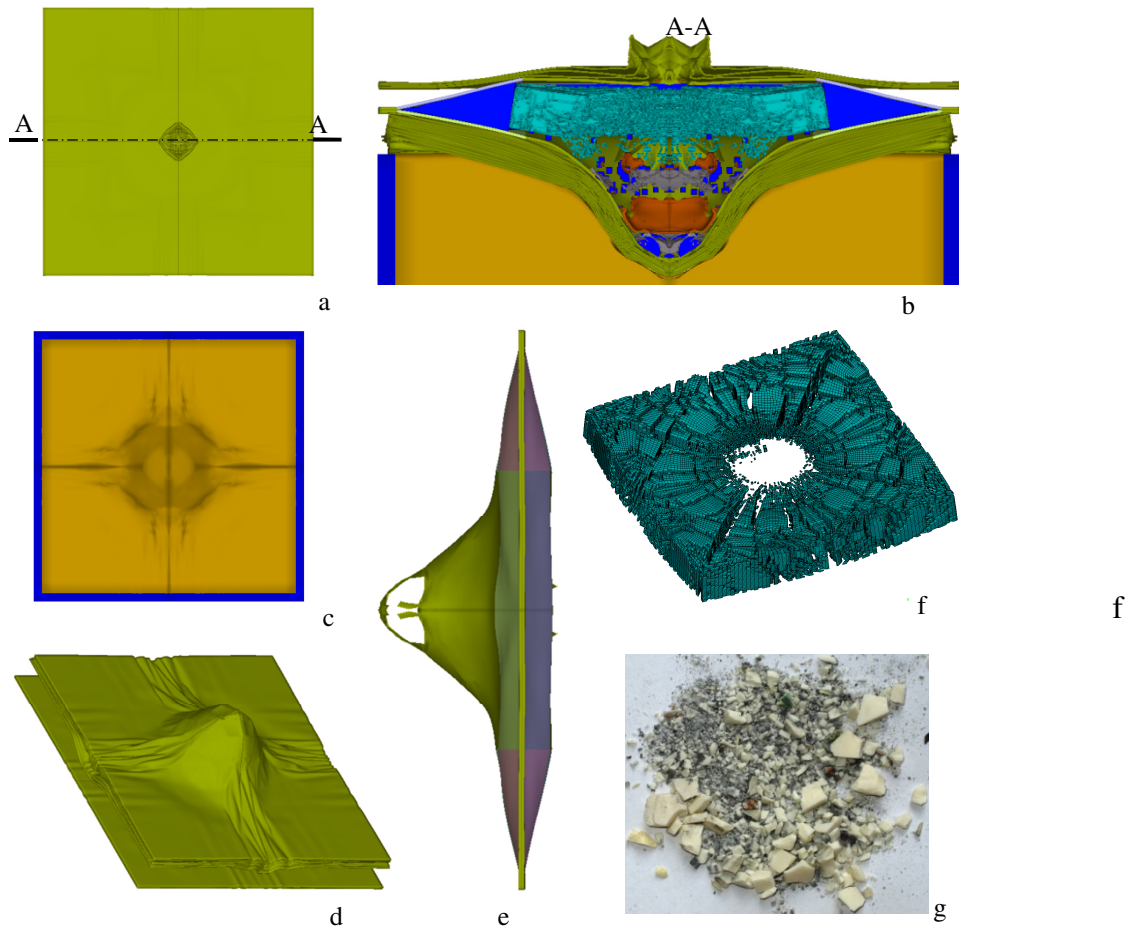


Fig. 13. Results of the numerical simulation: a – front view of the armour; b – cross-section of the armour, the projectile and the box with the backing material; c – the backing material; d – the aramid layers; e – the bag; f – the fragmented ceramic tile; the ballistic test result: g – the fragmented ceramic tile

All the armours variants with the Al_2O_3 ceramic tiles were perforated by the 5.56 × 45 mm SS109 projectile. The lowest residual velocity of the projectile (average velocity of the lead core) $V_{p \min} = 250$ m/s was achieved for the armour consisting of 3 mm thick Al_2O_3 ceramic tile and 2 mm thick Ti6Al4V plate (Figure 14).

Table 4. Areal densities of a final modular armour for investigated numerically material configurations and respective results, obtained in numerical simulations

		Armour areal density, m_{ma} , kg/m ²									
		Al ₂ O ₃ – 100 × 100 mm with thickness t , mm				SiC – 100 × 100 mm with thickness t , mm				Ti6Al4V – 100 × 100 mm with thickness t , mm	
1st layer	2nd layer	$t = 3$	$t = 4$	$t = 5$	$t = 6$	$t = 3$	$t = 4$	$t = 5$	$t = 6$	$t = 5$	$t = 4$
none				25.2 P	29.9 P			21.2 S	25.2 S	29.0 S	23.5 S
Armox 500 100 × 100 × 1 mm		25.4 P	30.1 P			22.9 P	27 S				
Ti6Al4V 100 × 100 × 1 mm			26 P	30.7 P			22.6 S	26.5 S			
Ti6Al4V 100 × 100 × 2 mm		26.7 P				24.2 S	28.1 S				

P – armour perforation; S – projectile stopping

In case of the armours for which the projectile stopping was achieved for its impact velocity $V_i = 900$ m/s, the numerical simulations for the projectile impact velocities $V_i = 950$ m/s and $V_i = 1000$ m/s were also performed. Values of the critical projectile velocity – the ballistic limit V_{50} (understood in this case as the minimal velocity at which the projectile perforates the armour) respectively to the obtained results were assigned to each armour in Table 5. Armours for which the areal density of the final modular armour would equal to $m_{ma} = 21.2 \div 24.2$ kg/m² in case of the 5.56 × 45 mm SS109 projectile impact velocity $V_i = 1000$ m/s were perforated.

Dependence of the projectile steel core and lead core velocities change in time for these armours is presented in Figure 15. Results of numerical simulations for armours, with areal densities equal to $m_{ma} = 25.2 \div 29.0$ kg/m² for which in case of the impact velocity $V_i = 1000$ m/s the projectile was stopped are shown in Figure 16.

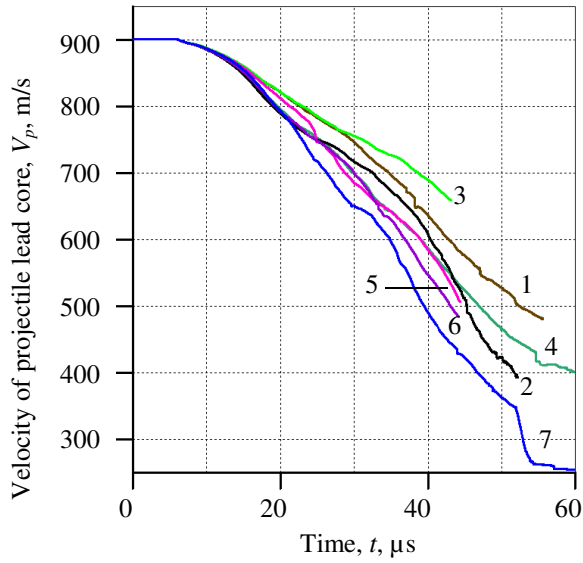


Fig. 14. Dependence between projectile velocity and time for different armour variants with the Al₂O₃ ceramic tile:

- 1 – 5 mm Al₂O₃; 2 – 6 mm Al₂O₃; 3 – 3 mm Al₂O₃ + 1 mm ArmoX 500;
- 4 – 4 mm Al₂O₃ + 1 mm ArmoX 500; 5 – 4 mm Al₂O₃ + 1 mm Ti6Al4V;
- 6 – 5 mm Al₂O₃ + 1 mm Ti6Al4V; 7 – 3 mm Al₂O₃ + 2 mm Ti6Al4V

Table 5. Ballistic limit V50 for the particular variants of armours

Thickness of layers, mm				Areal density for modular armour, m_{ma} , kg/m ²	Ballistic limit, V50, m/s			
Al ₂ O ₃	SiC	ArmoX 500	Ti6Al4V		< 900	900÷950	950÷1000	> 1000
5	-	-	-	25.2	x			
6	-	-	-	29.9	x			
3	-	1	-	25.4	x			
4	-	1	-	30.1	x			
4	-	-	1	26.0	x			
5	-	-	1	30.7	x			
3	-	-	2	26.7	x			
-	5	-	-	21.2			x	
-	6	-	-	25.2				x
-	4	1	-	27.0				x
-	3	1	-	22.9	x			
-	5	-	1	26.5				x
-	4	-	1	22.6		x		
-	4	-	2	28.1				x
-	3	-	2	24.2		x		
-	-	-	5	29.0				x
-	-	-	4	23.5		x		

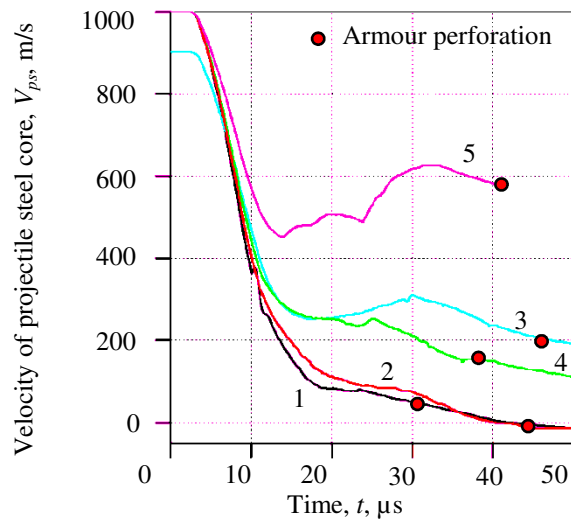
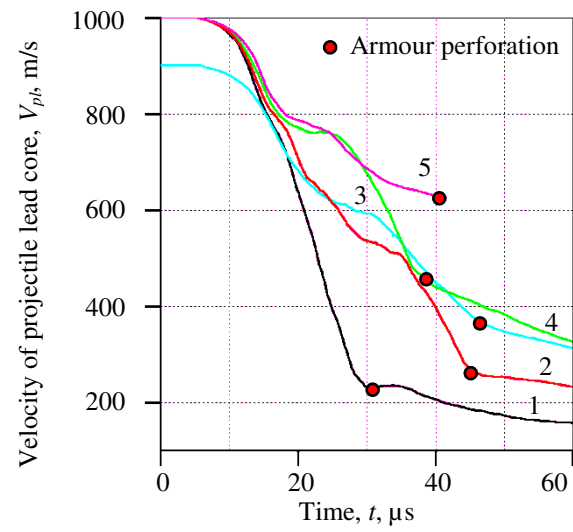


Fig. 15. Projectile steel core and lead core velocities in functions of time for different armours: 1 – 5 mm SiC; 2 – 4 mm SiC + 1 mm Ti6Al4V; 3 – 3 mm SiC + 1 mm ArmoX 500; 4 – 3 mm SiC + 2 mm Ti6Al4V; 5 – 4 mm Ti6Al4V

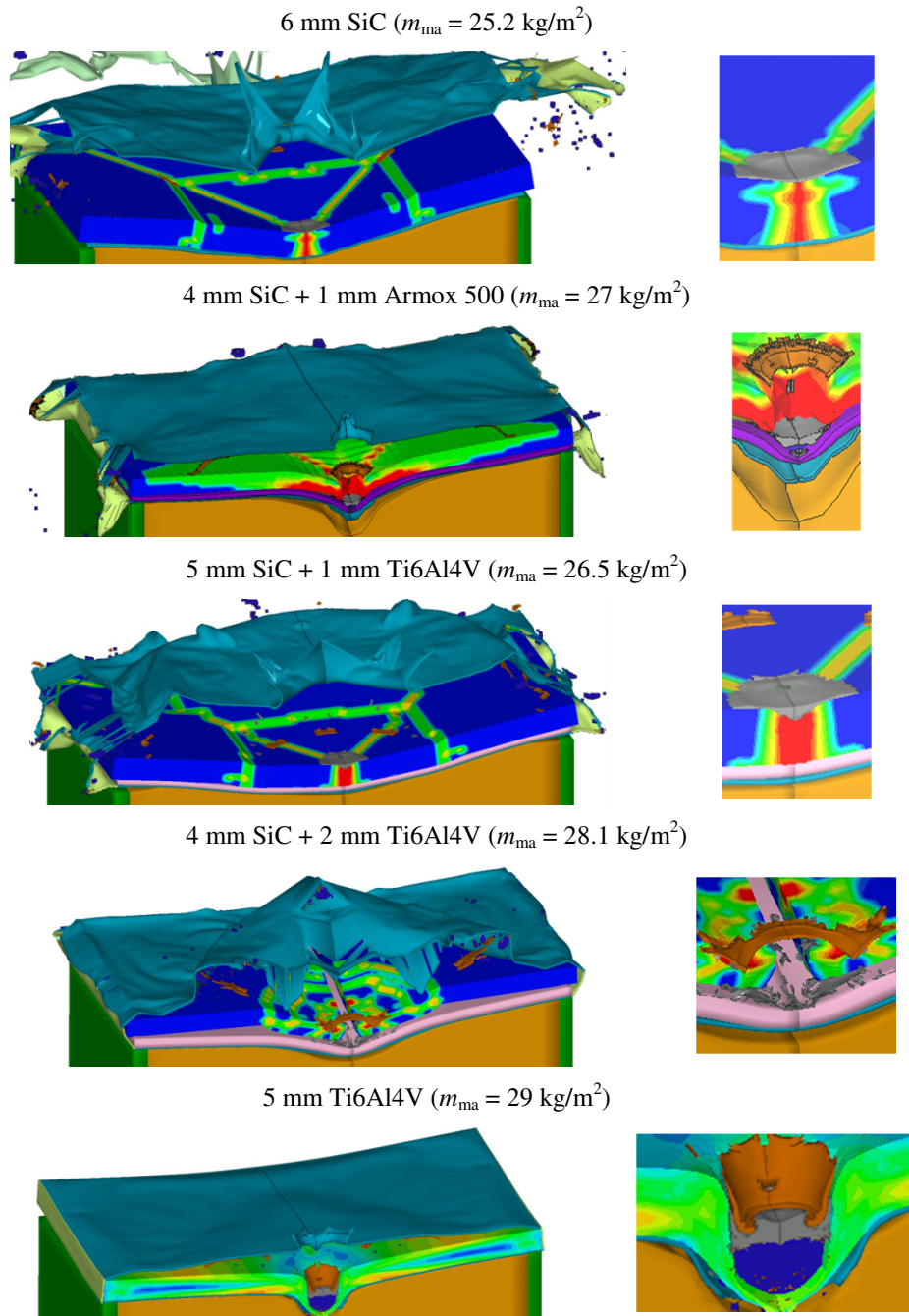


Fig. 16. Results of simulations of the 5.56 × 45 mm SS109 projectile impact onto the armours

Because the projectile of the highest investigated impact velocity $V_i = 1000$ m/s 5.56×45 mm SS109 was stopped by several variants of armours selection of the best armour variant was based on the armour damage. In each variant one-layer aramid bag made of Kevlar XP S307 was damaged by the jacket and steel core fragments penetration. Among the above mentioned group of armours as the most damaged and the less effective armour was recognized the armour with 5-mm thick titanium Ti6Al4V plate ($m_{ma} = 29$ kg/m²), where the lower bag layer was broken and the steel projectile core was not damaged, in difference to armours variants with SiC ceramic tiles. In the cases of 4-mm SiC tile added to 1 mm ArmoX 500 plate ($m_{ma} = 27$ kg/m²) and of 4 mm SiC tile added to 2-mm Ti6Al4V plate ($m_{ma} = 28.1$ kg/m²), the lead core of projectile was stopped on the layer behind the ceramic layer, causing its bulging. For armour with 2-mm Ti6Al4V, bulging was smaller. For titanium-ceramic armour the use of a thicker ceramic tile and a thinner titanium plate (5 mm SiC added to 1 mm Ti6Al4V) of lower areal density ($m_{ma} = 26.5$ kg/m²) appeared as more effective than the above mentioned solution, and the projectile stopping was obtained on the ceramic tile. In the case of the use of the 6 mm thick SiC ceramic tile ($m_{ma} = 25.2$ kg/m²), similar result was obtained but this variants requires application of appropriately resistant bag ensuring protection against the ceramic fragments.

4. CONCLUSIONS

On the basis of the ballistic tests and the numerical simulations the following conclusions can be drawn:

1. Advantages of the proposed armour over used now modern armours are as follows:
 - flexibility – yielding more freedom of movement for the user;
 - modularity – yielding the possibility of quick replacement of damaged armour elements.
2. Stopping of the 5.56×45 mm SS109 projectile with the use of the Al₂O₃ ceramic tiles with regards to the final modular armour is possible for relatively high areal density (42,1 kg/m²). In case of further study, the use of other ceramic tiles (e.g. SiC tiles) and other kind of materials (e.g. Ti6Al4V) is advisable.
3. In case of investigated numerically variants of armours, the most effective and practical solution for protection against the 5.56×45 mm SS109 projectile is the armour consisting of the 5-mm thick SiC ceramic tile and 1 mm thick titanium Ti6Al4V plate (areal density for modular armour $m_{ma} = 26.5$ kg/m²).
4. The aramid bag should be stuck together with other elements of the armour.

5. The numerically investigated one-layer aramid bag is not resistant enough and therefore it should be replaced by the multilayer aramid bag.

This work was financially supported by the European Fund for Regional Development in Poland (Project “Smart passive body armours with the use of rheological fluids with nano-structures” under the contract No. UDA-POIG.01.03.01-00-060/08-06) and carried out within consortium between the Institute of Security Technology „MORATEX” (Łódź, Poland), the Warsaw University of Technology (Warsaw, Poland) and the Military Institute of Armament Technology (Zielonka, Poland).

REFERENCES

- [1] Huta Stalowa Wola S.A Catalogue of products.
- [2] Brochure of Ceradyne, Inc. corporation: *Advanced Body Armor Systems*.
- [3] <http://www.concepteast.com/sinoarmor/sinoarmor-catalogue.pdf> (2014)
- [4] <http://www.vestguard.co.uk/downloads.htm> (2014).
- [5] Adams B., *Simulation on Ballistic Impacts on Armored Civil Vehicles*, Master Thesis, Eindhoven University of Technology, 2003.
- [6] Nsiampa N., Coghe F., Dyckmans G., *Numerical investigation of the bodywork effect (K-effect)*, DYMAT, pp. 1561-1566, 2009.
- [7] Hernandez V., Murr L., Anchondo I., Experimental observations and computer simulations for metallic projectile fragmentation and impact crater development in thick metal targets, *International Journal of Impact Engineering*, 32, pp. 1981-1989, 2006.
- [8] Krishnan K., Sockalingam S., Bansal S., Rajan S., Numerical simulation of ceramic composite armor subjected to ballistic impact, *Composites: Part B* 41, pp. 583-593, 2010.
- [9] Børvik T., Dey S., Clausen A., Perforation resistance of five different high-strength steel plates subjected to small-arms projectiles, *International Journal of Impact Engineering*, 36, pp. 948-964, 2009.
- [10] Johnson G., Cook W., A constitutive model and data for metals subjected to large strains, high strain rates and high temperatures, *Proceedings of the 7th International Symposium on Ballistics*, The Hague, Netherlands, pp. 541-547, 1983.
- [11] Wiśniewski A., Pacek D., Experimental research and numerical analysis of 9 mm Parabellum projectile penetration of ultra-high molecular weight polyethylene layers, *Problemy Techniki Uzbrojenia*, nr 3, s. 55-64, 2013.
- [12] Zduniak B., *Numeryczne badania doboru dwuwarstwowej osłony balistycznej*, rozprawa doktorska, Wojskowa Akademia Techniczna, Warszawa, s. 59, 2011.

- [13] Stanisławek S., *Badania odporności balistycznej niejednorodnych struktur ceramicznych*, rozprawa doktorska, Wojskowa Akademia Techniczna, Warszawa, s. 60, 62, 2014,
- [14] Morka A., Nowak J., Numerical analyses of ceramic/metal ballistic panels subjected to projectile impact, *Journal of KONES Powertrain and Transport*, vol. 19, no. 4, pp. 465-472, 2012.